HOKKAIDO UNIVERSITY

Title	Fabrication of porous (Ba,Sr)(Co,Fe)O3-delta (BSCF) ceramics using gelatinization and retrogradation phenomena of starch as pore-forming agent
Author(s)	Ishii, Kento; Shimizu, Makoto; Sameshima, Haruki et al.
Citation	Ceramics international, 46(9), 13047-13053 https://doi.org/10.1016/j.ceramint.2020.02.075
Issue Date	2020-06-15
Doc URL	https://hdl.handle.net/2115/84438
Rights	© 2020. This manuscript version is made available under the CC-BY-NC-ND 4.0 license http://creativecommons.org/licenses/by-nc-nd/4.0/
Rights(URL)	https://creativecommons.org/licenses/by-nc-nd/4.0/
Type	journal article
File Information	Manuscript_CI_R1_final accepted version.pdf

Original paper

Fabrication of Porous (Ba,Sr)(Co,Fe)O$_{3-\delta}$ (BSCF) Ceramics using Gelatinization and Retrogradation Phenomena of Starch as Pore Forming Agent

Kento Ishii[a,b], Makoto Shimizu[a,c], Haruki Sameshima[a,c], Sadaki Samitsu[d], Takamasa Ishigaki[c], Tetsuo Uchikoshi[a,b],*

[a] *Research Center for Functional Materials, National Institute for Material Science, 1-2-1 Sengen, Tsukuba, Ibaraki 305-0047, Japan*

[b] *Graduate School of Chemical Sciences and Engineering, Hokkaido University, Kita 8, Nishi 5, Kita-ku, Sapporo, Hokkaido, 060-0808, Japan*

[c] *Department of Chemical Science and Technology, Hosei University, 3-7-2 Kajinocho, Koganei, Tokyo, 184-8584, Japan*

[d] *Research Network and Facility Services Division, National Institute for Material Science, 1-2-1 Sengen, Tsukuba, Ibaraki 305-0047, Japan*

*Corresponding author.

Email address: UCHIKOSHI.Tetsuo@nims.go.jp (T. Uchikoshi)

Telephone number: +81-29-859-2460

Fax number: +81-29-859-2401

ABSTRACT

Porous (Ba,Sr)(Co,Fe)$O_{3-\delta}$ (BSCF) ceramics with high open porosity and good electrical conductivity was fabricated using $Ba_{0.5}Sr_{0.5}Co_{0.8}Fe_{0.2}O_{3-\delta}$ (BSCF), which shows a high mixed ionic-electronic conductivity. In general, during the fabrication of porous ceramics by the sacrificial template method using pore former particles, closed pores are easily formed unless sufficient pore former particles are added. In this study, we have devised a method using the gelatinization-retrogradation phenomena of starch for producing a porous body with an excellent percolated pore network structure. By dispersing BSCF and starch in an aqueous slurry (0-50% by weight) and heating, gelatinization of the starch occurred and the starch particles adhered to each other. Furthermore, in order to retain the percolated structure, the water solvent was removed by freeze-drying without heating to obtain a dried green body. The sintering behavior of the porous BSCF bodies prepared under various conditions was characterized by microstructural observations and relative density measurements. By optimizing the process conditions of the gelatinization and retrogradation, a porous body having an open porosity of 48.3%, and with 99% of the total pores open, was obtained. The matrix was also well connected and showed a sufficiently high conductivity which was similar to the porous bodies made by the traditional sacrificial template method.

2

Keywords:

1. Introduction

Porous ceramics are often used in various applications such as thermal insulation, adsorbents, filters, gas sensors, and catalyst supports[1]. In particular, a porous body using a mixed ionic-electronic conductor (MIEC) is used as an electrode of solid oxide electrochemical cells such as a solid oxide fuel cell or a porous support of an oxygen separation membrane. In these porous ceramics, it is very important to design the porosity, microstructure and mechanical properties according to the applications. In order to sufficiently promote the electrode reaction, the MIEC porous body must have a percolated network structure in which raw materials, such as a reaction gas, can easily reach the surface of the electrolyte or separation membrane layer[2–4]. Moreover, it must have a large specific surface area as a reaction field. Typical fabrication processes for macroporous ceramics include partial sintering, sacrificial templates, replica templates and direct foaming. In addition to these fabrication processes, many new approaches for macroporous ceramics, such as phase separation and three-dimensional printing (3D printing), have been developed[1,5–9].

To fabricate oxygen separation membranes with an asymmetric structure, thin layers are usually prepared on porous supports by tape casting, screen printing, dip coating and spin coating [10]. The method for preparing a porous body using phase inversion of

polymer is a promising method that can be applied to the production of ceramic asymmetric membranes in a single step at a low cost. However, the phase inversion method involves many processing parameters that need to be optimized during the manufacturing process, so controlling film thickness and structure is not easy[11–13]. Tape casting is commonly used to produce homogeneous free-standing films but is not suitable for producing asymmetric films. In addition to these methods, perovskite foaming has been reported as a method for preparing porous materials[1,14,15]. In particular, sacrificial template method[3,16–19], tape casting method[2,4,20–23], phase inversion method[24], and freeze-drying method[25] have been reported for the fabrication method of porous BSCF.

For the fabrication of a conventional porous body, like the sacrificial template method, a mixed powder in which pore-forming agent particles are uniformly dispersed in a matrix material, is shaped, followed by removal of the pore-forming agent before, during or after sintering of the matrix material. A wide variety of sacrificial materials have been used as pore formers, including natural and synthetic organics, salts, liquids, metals, and ceramic compounds[9]. However, even if the pore forming agent material is uniformly dispersed in the matrix material, closed pores are generally formed if the amount of the pore-forming material is not sufficient as shown in Fig. 1(a).

Many porous ceramics using starch powders as a pore forming agent have been reported[4,26,35,36,27–34]. In the conventional method, various plant-derived starch particles suitable for the target pore shape have been used in their original states. By using starch particles as a pore-forming material, a good porous body without any residue can be obtained by firing at about 500 °C. However, simply using starch powder as a substitute for polymer beads, such as polystyrene and PMMA, is not always a good method to form a percolated pore network.

Starch is a polysaccharide composed of amylose and amylopectin produced by the photosynthesis of plants, and is a granular solid, and the ratio and shape of the particles differ depending on the type of plant. Figure 2 shows a schematic illustration of the gelatinization and retrogradation of starch[37–42]. The amylose and amylopectin fractions become loose during heating and in the presence of excess water, and these fractions start to solubilize at 70°C and 90°C, respectively. Starch granules initially absorb water causing them to gradually swell and form a viscous slurry. As heating continues and the temperature increases, the granules start losing their crystallinity and become amorphous. Subsequent heating causes the granules size to increase until they can no longer absorb more water and burst. As molecules making up the granule start to leach out from the swollen granules and disperse/solubilize in the aqueous medium, they yield a gel or paste whose properties depend

on the concentration and type of the starch. Retrogradation begins immediately after stopping the heating. Retrogradation of the amylopectin is a slow process, on the other hand, amylose retrogrades very quickly during cooling. The gelatinized starch then starts to cool to ambient temperature and solidifies, leading to water separation and molecular realignment. Retrogradation is associated with recrystallization of the starch molecules.

When an aqueous slurry in which starch powder, which is a pore-forming agent, and the matrix material powder are dispersed, is heated, the starch is gelatinized and connected to each other. This starch consolidation technique has been reported in which the starch powder is swollen by heating a mixture of starch and matrix material in an aqueous slurry to form a connected pore network [43–49]. We have recently devised a method for fabricating a porous support using the gelatinization and successive retrogradation phenomena of starch. We postulated that it would be possible to produce porous materials with an excellent pore connectivity using these phenomena as shown in Fig.1 (b). The purpose of this study is to produce a porous material with an excellent pore connectivity and electrical conductivity based on the $(Ba,Sr)(Co,Fe)O_{3-\delta}$ (BSCF) mixed conductor by utilizing the gelatinization-retrogradation phenomena of starch.

2. Materials and methods

Figure 3 shows a schematic illustration explaining the preparation procedure of the porous bodies. Five vol% of $Ba_{0.5}Sr_{0.5}Co_{0.8}Fe_{0.2}O_{3-\delta}$ (BSCF) powder (Kusaka Rare Metal Products Co., Ltd.) with an average particle size of 0.5 µm was added to distilled water. Next, rice starch powder (Sigma-Aldrich Co. LLC) with the particle size range of 2.0−8.0 µm was added to the slurry in an amount of 25 wt% versus the BSCF powder. The mixed slurry was deflocculated using an ultrasonic homogenizer. Next, the resulting slurry was heated and stirred at about 65 °C for 1 h using a hot stirrer to gelatinize the rice starch in the slurry. This slurry was poured into an acrylic cylindrical container standing on a metal plate, then the sample was cooled in a refrigerator at 0±2 °C for 2h to accelerate the retrogradation and the exudation of moisture in the gelatinized starch. Furthermore, the sample was gradually frozen at −18 °C or rapidly frozen at −196 °C with liquid nitrogen, then freeze-dried under a reduced pressure of 10 Pa to obtain green bodies. Figure 4 shows SEM micrographs of (a) the as-received starch powder, (b) the gelatinized starch after freeze-drying, and (c) retrograded starch after freeze-drying. The sacrificial templates of the starch, like these images, would be formed. Thereafter, the green bodies were fired at 900 °C or 1100 °C for 3 hours to produce the BSCF porous bodies. The porosity of the green bodies and porous bodies were measured by the Archimedes' method in kerosene. The microstructures of the sample were observed by scanning electron microscopy (SEM) using a field-emission SEM (JEOL, JSM-6510) and a

tabletop-SEM (Hitachi, TM-3000). The electrical conductivity of the porous bodies sintered

at 1100 °C was evaluated by the DC 2-terminal method using a source meter (Keithley, model

2400).

3. Results and discussion

Fig. 5 shows the microstructure of the green bodies after freeze-drying. Table 1 shows the

retrogradation progress, porosity and the apparent pore size of each sample. The green body

(Fig. 5 (a)), which was rapidly frozen at −196 °C and vacuum freeze-dried with no

retrogradation treatment, showed an open porosity of 57.6%. The green body (Fig. 5 (b)),

which was rapidly frozen at −196 °C and vacuum freeze-dried with the retrogradation

treatment, showed an open porosity of 77.6%, and the pore size range was 5.0−10.0 µm. The

green body (Fig. 5 (c)), which was slowly frozen at −18 °C and vacuum freeze-dried with the

retrogradation treatment, showed an open porosity of 87.8%, and the pore size range was

10.0−50.0 µm.

In the rapidly frozen and then freeze-dried samples (Figure 5 (a) and (b)), a difference in

the microstructure of the green bodies was observed depending on whether aging was

promoted. This is probably because the exuded water from the gelatinized starch was frozen

during the retrogradation process, and voids were formed by the ice crystals sublimating by

9

the freeze drying. In addition, in the rapidly frozen and slowly frozen samples followed by the retrogradation treatment (Figure 5 (b) and (c)), a difference in the microstructure of the green bodies was also observed depending on whether aging was promoted. This is likely because in the case of the slow freeze, not only the exudate during the retrogradation treatment, but more water will be exuded during the subsequent freezing process. When the sample is rapidly frozen at liquid nitrogen temperature, the time for water exudation from the gelatinized tissue is extremely short, and the amount of water to be exuded is relatively small, resulting in the formation of fine ice crystals, thus smaller pores. On the other hand, the freezing rate of water at −18 °C is slow, therefore, there is sufficient time for more water to exudate out, resulting in the formation of large ice crystals and consequently coarse pores.

Figures 6 (a-c) and (A-C) show SEM images of the fractured surfaces of the porous bodies produced by firing the green bodies of Figs. 5 (a) to (c) at 900 °C or 1100 °C, respectively. Figure 6 (A'-C') are the wide-area images of Figure 6 (A-C). The sample prepared by firing the green body at 900 °C is not shown here because the sample was too brittle to observe the microstructure. When the porous body shown in Fig. 5 (c) was fired at 1100 °C (Fig. 6 (C)), a high open porosity was obtained, but the brittleness was not improved. When the rapidly frozen compacts shown in Figs. 6 (a) and (b) were fired at 900 °C, the pores were uniformly distributed and favorably connected regardless of the retrogradation treatment as shown in

Figs.6 (a) and (b). In the porous bodies fired at 1100 °C, it was observed that the sample with

the non-retrogradation treatment (Fig. 6(A)) had a significantly reduced porosity compared

to the other samples (Fig. 6(B) and (C)). This is probably because the sintering between the

particles progressed as the firing temperature increased, and the pores of 0.5−5.0 μm in size,

which were observed in the porous body fired at 900 °C, shrunk, and the connected structure

was lost. On the other hand, in the porous body that was retrograded, then fired at 900 °C,

the pores of 5.0−10 μm size were maintained as shown in Fig. 6(b). Furthermore, even at the

1100 °C firing, connected pores having a range of 2.0−8.0 μm were retained as shown in Figs.

6(B) and (C). Based on these results, it is considered that the pore size of the retrograded

sample increased due to the more exuding from the gelatinized starch, resulting in the

formation of coarse pores as compared to the non-gelatinized sample.

Figure 7 shows the microstructure of (a) the dense body produced by the uniaxial pressure

molding method, (b) the porous body by the conventional method, and (c) the porous body by

freeze drying followed by firing at 1100 °C. Table 2 shows the porosity, apparent pore size,

and electrical conductivity of each sample. Porous bodies prepared by this technique have a

pore size similar to that of the conventional methods, but have a higher porosity, and 99% of

the total pores are open pores. The electrical conductivity of the porous body obtained by this

method was similar to that of the porous body prepared by the conventional method, and the

connectivity of the matrix was sufficiently high as well as the connectivity of the pores.

In general, the pore structure is evaluated by gas adsorption, mercury intrusion, and X-ray CT. In the pore distribution measurement by the gas adsorption method, the range in which the pores can be measured is 0.1 to 100 nm, which is not suitable for the measurement of the pore diameter of the porous BSCF prepared in this study. In the mercury intrusion method, pores with a diameter of several nm to several hundred µm are measured. However, in this method, a cylindrical pore is a measurement target and is not suitable for the measurement of a three-dimensional network structure in which many pores are connected. Therefore, we tried to observe the pore structure of the sample by X-ray CT. Although the maximum measurable resolution of the instrument was 5 µm, observation of the pore structure of this sample was difficult, and visualization of the pore shape and three-dimensional network structure was not possible.

To confirm that the fabricated porous BSCF has excellent pore connectivity, a high-precision specific surface area measurement using krypton gas was performed. The specific surface area measurement results were: 0.24 m2 / g for rapidly frozen samples without retrogradation treatment (Fig.6 (A)), 0.27 m2 / g for rapidly frozen samples with retrogradation treatment (Fig.6(B)), 0.07 m2 / g for samples prepared by the sacrificial template method (Fig.7 (c)), 8.6 m2 / g for BSCF raw powder. The specific surface area in

which the porous bodies produced by utilizing the gelatinization and retrogradation phenomena after sintering (Fig.6 (A and B)) were smaller than that of the raw powder. However, the specific surface area of these porous bodies was 3 to 4 times higher than that of the porous body prepared by the sacrificial template method (Fig.7 (c)). Further, the sample of Fig.6 (B) with retrogradation treatment had a higher specific surface area than the sample of Fig.6 (A) without no retrogradation treatment. This suggests that the sample in Fig. 6(B) has a high open porosity, which is consistent with the porosity measurements.

The wide-area SEM image shown in Fig. 6 (A'-C') exhibits that the porous bodies produced by utilizing the gelatinization and retrogradation phenomena have a highly connective pore structure. These results of specific surface area measurement, porosity measurement, and SEM observation show that the porous body formed by using the gelatinization and retrogradation phenomena forms a network structure with a highly connective pore structure.

Figure 8 shows the relationship between the porosity and the firing temperature of the porous materials prepared under different conditions. The porosity of the non-retrograded sample increased due to the 900 °C firing and decreased at 1100 °C. Considering that the burnout temperature of starch is around 500 °C and the starting temperature of the sintering of BSCF is around 900 °C, the reason why the porosity increased by firing at 900 °C is probably because the densification does not significantly progress. At the firing temperatures

of 1000 °C or higher, the densification further proceeds, so that the pores diminish and the porosity decreases. On the other hand, the porosity of the retrograded sample slightly decreased at 900 °C, and further decreased by firing to 1100 °C. This is probably because the coarse pores hinder the sintering progress of the matrix.

In this study, rice-derived starch was used, but using starch from other plants with different ratios of amylose and amylopectin would result in the formation of pores with different tissue structures. The method of producing a porous body using the gelatinization-retrogradation phenomena of starch is a promising method with excellent environmental compatibility for producing a porous body with excellent connectivity, which can be applied to other matrix materials.

4. Conclusions

A new processing method for producing porous materials has been proposed by selecting the combination of rice starch and BSCF; i.e., starch powder as a pore-forming agent is gelatinized to connect them together and promote the appropriate retrogradation phenomenon to freeze the exuded water, and subsequent vacuum freeze-drying the ice crystal and firing. Consequently, connected pores having a pore diameter such that pores formed later would not disappear due to heat shrinkage are formed, and a porous body of BSCF

having an excellent open porosity is produced.

References

[1]   T. Ohji, M. Fukushima, Macro-porous ceramics : processing and properties, Int.

        Mater. Rev. 57 (2012) 115–131. doi:10.1179/1743280411Y.0000000006.

[2]   P. Niehoff, S. Baumann, F. Schulze-Küppers, R.S. Bradley, I. Shapiro, W.A.

        Meulenberg, P.J. Withers, R. Vaßen, Oxygen transport through supported

        Ba0.5Sr0.5Co 0.8Fe0.2O3-δ membranes, Sep. Purif. Technol. 121 (2014) 60–67.

        doi:10.1016/j.seppur.2013.07.002.

[3]   P.L. Rachadel, J. Motuzas, G. Ji, D. Hotza, J.C. Diniz da Costa, The effect of non-

        ionic porous domains on supported Ba0.5Sr0.5Co0.8Fe0.2O3-δ membranes for O2

        separation, J. Memb. Sci. 454 (2014) 382–389. doi:10.1016/j.memsci.2013.11.054.

[4]   F. Schulze-Küppers, S. Baumann, W.A. Meulenberg, D. Stöver, H.P. Buchkremer,

        Manufacturing and performance of advanced supported Ba0.5Sr0.5Co0.8Fe0.2O3-δ

        (BSCF) oxygen transport membranes, J. Memb. Sci. 433 (2013) 121–125.

        doi:10.1016/j.memsci.2013.01.028.

[5]   D.D. Athayde, D.F. Souza, S.A. M.A., Review of perovkite ceramic synthesis and

        membrane preparation methods, Ceram. Int. 42 (2016) 6555–6571.

        doi:10.1016/j.ceramint.2016.01.130.

[6]   R.K. Nishihora, P.L. Rachadel, M.G.N. Quadri, D. Hotza, Manufacturing porous

ceramic materials by tape casting—A review, J. Eur. Ceram. Soc. 38 (2018) 988–

1001. doi:10.1016/j.jeurceramsoc.2017.11.047.

[7]   N. Sarkar, I.J. Kim, Porous Ceramics, in: A.M.. Mohamed (Ed.), Adv. Ceram.

Process., IntechOpen, 2015: pp. 55–84.

[8]   U.M. Basheer, A Brief Introduction to Porous Ceramic, in: U.M. Basheer (Ed.),

Recent Adv. Porous Ceram., IntechOpen, 2018: pp. 1–10. doi:10.5772/68104.

[9]   R. Studart, U.T. Gonzenbach, E. Tervoort, L.J. Gauckler, Processing Routes to

Macroporous Ceramics: A Review, J. Am. Ceram. Soc. 89 (2006) 1771–1789.

doi:10.1111/j.1551-2916.2006.01044.x.

[10]   P. Lemes-Rachadel, G.S. Garcia, R.A.F. Machado, D. Hotza, J.C.D. da Costa,

Current developments of mixed conducting membranes on porous substrates, Mater.

Res. 17 (2014) 242–249. doi:10.1590/S1516-14392013005000175.

[11]   G.R. Guillen, Y. Pan, M. Li, E.M. V Hoek, Preparation and Characterization of

Membranes Formed by Nonsolvent Induced Phase Separation : A Review, Ind. Eng.

Chem. Res. 50 (2011) 3798–3817. doi:10.1021/ie101928r.

[12]   H. Fang, C. Ren, Y. Liu, D. Lu, L. Winnubst, C. Chen, Phase-inversion tape casting

and synchrotron-radiation computed tomography analysis of porous alumina, J. Eur.

Ceram. Soc. 33 (2013) 2049–2051. doi:10.1016/j.jeurceramsoc.2013.02.032.

[13]   W. He, H. Huang, J. Gao, L. Winnubst, C. Chen, Phase-inversion tape casting and oxygen permeation properties of supported ceramic membranes, J. Memb. Sci. 452 (2014) 294–299. doi:10.1016/j.memsci.2013.09.063.

[14]   P. Colombo, J.R. Hellmann, Ceramic foams from preceramic polymers, (2002) 260–272. doi:10.1007/s10019-002-0209-z.

[15]   P. Ge, A. Vivet, L. Guironnet, N. Richet, F. Rossignol, T. Chartier, Perovskite foams used in combination with dense ceramic membranes for oxygen transport membrane applications, 44 (2018) 19831–19835. doi:10.1016/j.ceramint.2018.07.241.

[16]   D.A. Slade, Q. Jiang, K.J. Nordheden, S.M. Stagg-Williams, A comparison of mixed-conducting oxygen-permeable membranes for CO2 reforming, Catal. Today. 148 (2009) 290–297. doi:10.1016/j.cattod.2009.08.016.

[17]   A. V. Kovalevsky, A.A. Yaremchenko, V.A. Kolotygin, A.L. Shaula, V. V. Kharton, F.M.M. Snijkers, A. Buekenhoudt, J.R. Frade, E.N. Naumovich, Processing and oxygen permeation studies of asymmetric multilayer Ba0.5Sr0.5Co0.8Fe0.2O3-δ membranes, J. Memb. Sci. 380 (2011) 68–80. doi:10.1016/j.memsci.2011.06.034.

[18]   X. Cui, R. O'Hayre, S. Pylypenko, L. Zhang, L. Zeng, X. Zhang, Z. Hua, H. Chen, J. Shi, Fabrication of a mesoporous Ba0.5Sr0.5Co0.8Fe0.2O3-: δ perovskite as a low-cost and efficient catalyst for oxygen reduction, Dalt. Trans. 46 (2017) 13903–13911.

doi:10.1039/c7dt03082g.

[19]   B. He, D. Ding, Y. Ling, J. Xu, L. Zhao, Efficient modification for enhancing surface

         activity of Ba0.5Sr0.5Co0.8Fe0.2O3-δoxygen permeation membrane, J. Memb. Sci.

         477 (2015) 7–13. doi:10.1016/j.memsci.2014.12.020.

[20]   M. Lipinska-Chwalek, J. Malzbender, A. Chanda, S. Baumann, R.W. Steinbrech,

         Mechanical characterization of porous Ba0.5Sr0.5Co0.8Fe0.2O3-d, J. Eur. Ceram.

         Soc. 31 (2011) 2997–3002. doi:10.1016/j.jeurceramsoc.2011.07.002.

[21]   S. Baumann, J.M. Serra, M.P. Lobera, S. Escolástico, F. Schulze-Küppers, W.A.

         Meulenberg, Ultrahigh oxygen permeation flux through supported

         Ba0.5Sr0.5Co0.8Fe0.2O3-δmembranes, J. Memb. Sci. 377 (2011) 198–205.

         doi:10.1016/j.memsci.2011.04.050.

[22]   X. Li, T. Kerstiens, T. Markus, Oxygen permeability and phase stability of

         Ba0.5Sr0.5Co0.8Fe0.2O3-δ perovskite at intermediate temperatures, J. Memb. Sci.

         438 (2013) 83–89. doi:10.1016/j.memsci.2013.03.017.

[23]   M. Lipinska-Chwalek, F. Schulze-Küppers, J. Malzbender, Stability aspects of

         porous Ba0.5Sr0.5Co 0.8Fe0.2O3-δ, Ceram. Int. 40 (2014) 7395–7399.

         doi:10.1016/j.ceramint.2013.12.085.

[24]   A. Kovalevsky, C. Buysse, F. Snijkers, A. Buekenhoudt, J. Luyten, J. Kretzschmar,

S. Lenaerts, Oxygen exchange-limited transport and surface activation of

Ba0.5Sr0.5Co0.8Fe0.2O3-δ capillary membranes, J. Memb. Sci. 368 (2011) 223–232.

doi:10.1016/j.memsci.2010.11.034.

[25]   P.L. Rachadel, D.F. Souza, E.H.M. Nunes, J.C.D. da Costa, W.L. Vasconcelos, D.

Hotza, A novel route for manufacturing asymmetric BSCF-based perovskite

structures by a combined tape and freeze casting method, J. Eur. Ceram. Soc. 37

(2017) 5249–5257. doi:10.1016/j.jeurceramsoc.2017.04.035.

[26]   M.M. Lorente-Ayza, M.J. Orts, V. Pérez-Herranz, S. Mestre, Role of starch

characteristics in the properties of low-cost ceramic membranes, J. Eur. Ceram. Soc.

35 (2015) 2333–2341. doi:10.1016/j.jeurceramsoc.2015.02.026.

[27]   M.N. Islam, W. Araki, Y. Arai, Ferroelastic mechanical behaivior of porous

La0.6Sr0.4Co0.2Fe0.8O3-δ prepared using corn starch as a pore former, Int. J.

Mech. Prod. Eng. 6 (2018) 37–40.

[28]   H. Itoh, H. Asano, M. Nagata, H. Iwahara, Preparation of CaTiO3 Porous Substrate

by Foam-Burning Method, J. Ceram. Soc. Japan. 105 (1997) 1022–1026.

[29]   E. Gregorová, Z. Živcová, W. Pabst, Porosity and pore space characteristics of starch-

processed porous ceramics, J. Mater. Sci. 41 (2006) 6119–6122. doi:10.1007/s10853-

006-0475-z.

[30]   Z. He, K.B. Andersen, L. Keel, F.B. Nygaard, M. Menon, K.K. Hansen, Processing

and characterization of porous electrochemical cells for flue gas purification, Ionics

(Kiel). 15 (2009) 427–431. doi:10.1007/s11581-008-0286-0.

[31]   R. Ahmad, M.S. Anwar, J. Kim, I.H. Song, S.Z. Abbas, S.A. Ali, F. Ali, J. Ahmad, H.

Bin Awais, M. Mehmood, Porosity features and gas permeability analysis of bi-modal

porous alumina and mullite for filtration applications, Ceram. Int. 42 (2016) 18711–

18717. doi:10.1016/j.ceramint.2016.09.009.

[32]   P. Albano, L.B. Garrido, K. Plucknett, L.A. Genova, Processing of porous yttria-

stabilized zirconia tapes : Influence of starch content and sintering temperature,

Ceram. Int. 35 (2009) 1783–1791. doi:10.1016/j.ceramint.2008.10.003.

[33]   E. Gregorová, Z. Živcová, W. Pabst, Porous Ceramics Made Using Potato Starch as a

Pore-forming Agent, Fruit, Veg. Ceram. Sci. Biotechnol. 3 (2009) 115–127.

[34]   L. Nie, J. Liu, Y. Zhang, M. Liu, Effects of pore formers on microstructure and

performance of cathode membranes for solid oxide fuel cells, J. Power Sources. 196

(2011) 9975–9979. doi:10.1016/j.jpowsour.2011.08.036.

[35]   B. Qifu, D. Weixia, Z. Jianer, W. Yongqing, L. Yang, Effects of Pore Former on

Properties of Alumina Porous Ceramic for Application in Micro-Filtration Membrane

Supports, Key Eng. Mater. 655 (2015) 97–102.

doi:10.4028/www.scientific.net/KEM.655.97.

[36] Y. Zhang, J. Zhu, H. Ren, Y. Bi, L. Zhang, Synthesis and properties of melamine–

      starch hybrid aerogels cross-linked with formaldehyde, J. Sol-Gel Sci. Technol. 83

      (2017) 44–52. doi:10.1007/s10971-017-4375-2.

[37] T.J. Schoch, Mechano-chemistry of Starch, Mechano-Chemistry of Starch. 14 (1967)

      53–78.

[38] T. Kuge, On the Physicochemical Properties of Starch, Denpun Kagaku. 39 (1992)

      51–56.

[39] T. Harada, A. Harada, Gel Formation and Ultrastructure in Food Ploysaccharides,

      MARCEL DEKKER, 1998.

[40] P. Taggart, Starch as an ingredient: manufacture and applications, in: A. ‐ C

      ELIASSON (Ed.), Starch Food, Woodhead Publishing Limited, CRC Press LLC,

      2004.

[41] H.F. Zobel, S. M., Starch: Structure, Analysis, and Application, in: A.M. Stephen,

      G.O. Phillips, P.A. Williams (Eds.), Food Polysaccharides Their Appl., Second Edi,

      Taylor & Francis, 2006: pp. 25–86.

[42] E. Gregorová, W. Pabst, I. Bohačenko, Characterization of different starch types for

      their application in ceramic processing, J. Eur. Ceram. Soc. 26 (2006) 1301–1309.

doi:10.1016/j.jeurceramsoc.2005.02.015.

[43] Z. Nie, Y. Lin, Fabrication of porous alumina ceramics with corn starch in an easy and low-cost way, Ceram. - Silikaty. 50 (2015) 348–352. doi:10.1115/DETC2012-71473.

[44] E. Gregorová, W. Pabst, Porosity and pore size control in starch consolidation casting of oxide ceramics-Achievements and problems, J. Eur. Ceram. Soc. 27 (2007) 669–672. doi:10.1016/j.jeurceramsoc.2006.04.048.

[45] L.B. Garrido, M.P. Albano, L.A. Genova, K.P. Plucknett, Influence of starch type on characteristics of porous 3Y-ZrO2 prepared from a direct consolidation casting method, Mater. Res. 14 (2011) 39–45. doi:10.1590/S1516-14392011005000016.

[46] M.L. Sandoval, M.H. Talou, P.M. De Souto, R.H.G.A. Kiminami, M.A. Camerucci, Microwave sintering of cordierite precursor green bodies prepared by starch consolidation, Ceram. Int. 37 (2011) 1237–1243. doi:10.1016/j.ceramint.2010.11.041.

[47] S. Li, C. Wang, J. Zhou, Effect of starch addition on microstructure and properties of highly porous alumina ceramics, Ceram. Int. 39 (2013) 8833–8839. doi:10.1016/j.ceramint.2013.04.072.

[48] Z. Živcová, E. Gregorová, W. Pabst, Alumina ceramics prepared with new pore-forming agents, Process. Appl. Ceram. 2 (2008) 1–8. doi:10.2298/PAC0801001Z.

[49]   O. Lyckfeldt, J.M.F. Ferreira, Processing of porous ceramics by 'starch consolidation,'

J. Eur. Ceram. Soc. 18 (1998) 131–140. doi:10.1016/S0955-2219(97)00101-5.

Figure and table captions

Fig. 1. Schematic illustrations showing the preparation of a porous body by the sacrificial template method: (a) common method, (b) method using the gelatinization-retrogradation phenomena of starch.

Fig. 2. Schematic illustrations of the gelatinization and retrogradation phenomena of starch.

Fig. 3. Preparation procedure of porous body of BSCF using rice starch as the pore forming agent.

Fig. 4. SEM images of (a) as-received rice starch powder, (b) freeze-dried gelatinized starch and (c) freeze-dried retrograded starch.

Fig. 5. Microstructures of the green bodies after freeze-drying (a-c): (a) no retrogradation treatment + rapid freezing, (b) retrogradation treatment + rapid freezing, and (c) retrogradation treatment + slow freezing.

Fig. 6. Microstructures of the porous bodies fired at 900 ˚C (a-b) and 1100 ˚C (A-C): (a, A) no retrogradation treatment + rapid freezing, (b, B) retrogradation treatment + rapid freezing, and (c, C) retrogradation treatment + slow freezing. A'-C' are the wide-area images of A-C.

Fig. 7. Microstructures of the BSCFs sintered at 1100 ˚C via different preparation methods: (a) uniaxial pressing without pore forming agent, (b) common sacrificial template

method, and (c) method using the gelatinization-retrogradation phenomena of starch (retrogradation treatment + rapid freezing). The added amounts of starch in (b) and (c) are both 25 wt%.

Fig. 8. Sintering properties of the BSCFs: (upper side) Relative density of BSCF with no starch prepared by uniaxial pressing; (lower side) open porosity of the sintered bodies prepared by different methods and conditions.

Table 1. The degree of retrogradation progress, porosity and the pore size of green bodies after freeze-drying: (a) no retrogradation treatment + rapid freezing, (b) retrogradation treatment + rapid freezing, and (c) retrogradation treatment + slow freezing.

Table 2. Porosity, open porosity, pore size, and electrical conductivity of the BSCFs sintered at 1100 ° C via different preparation methods: (a)uniaxial pressing without pore forming agent, (b) common sacrificial template method, and (c) method using the gelatinization-retrogradation phenomena of starch (retrogradation treatment + rapid freezing). The added amounts of starch in (b) and (c) are both 25 wt.%.

Fig.1
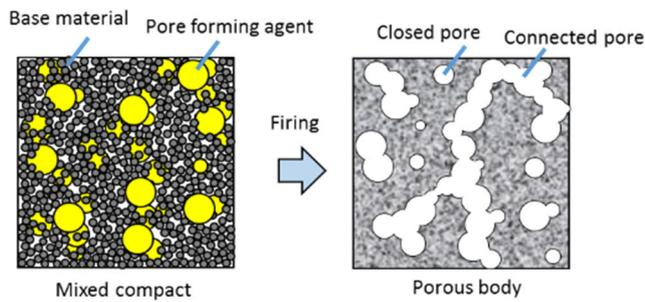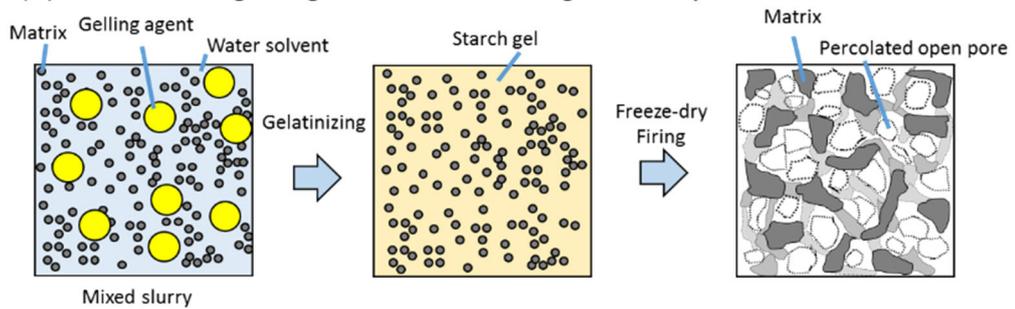
Fig. 1.   Schematic illustrations showing the preparation of a porous body by the sacrificial template method
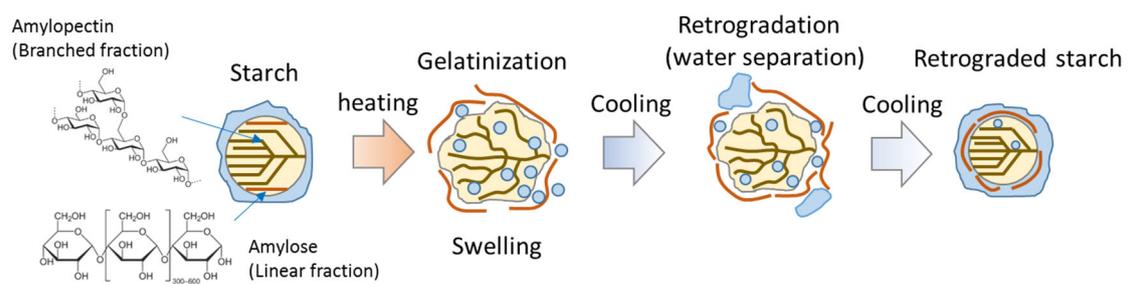
Fig.2

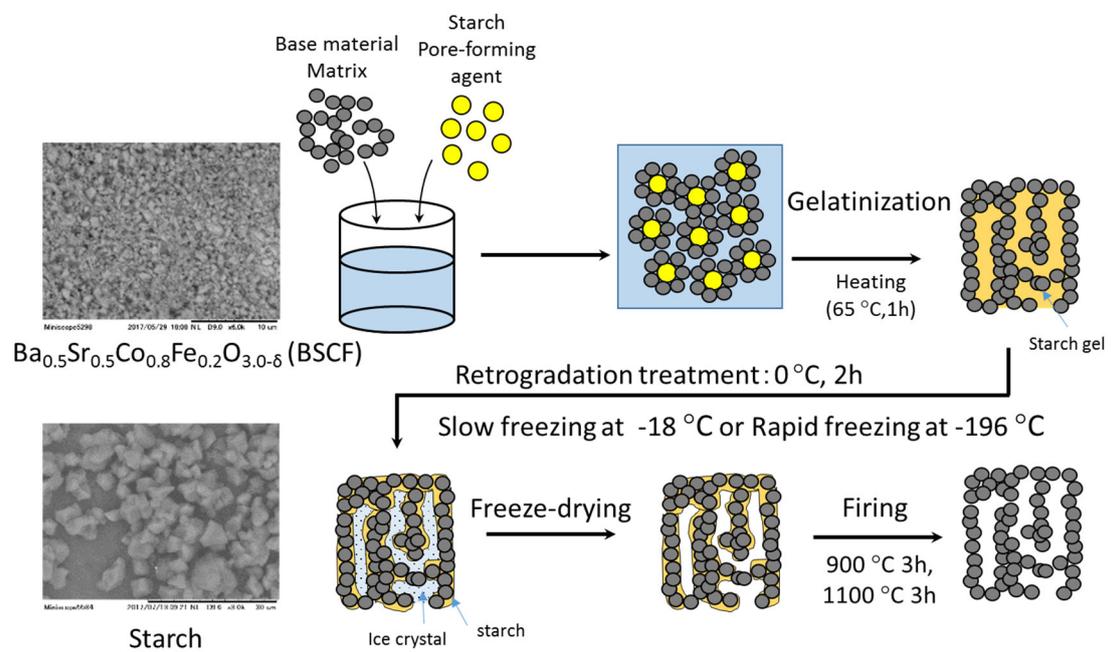Fig. 2.　Phenomena of starch gelatinization and retrogradation

Fig.3

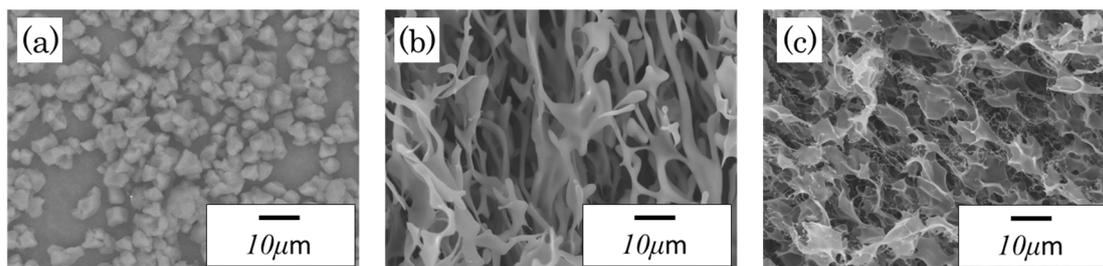Fig. 3. Preparation procedure of porous body of BSCF using rice starch as the pore forming agent.

Fig.4

Fig. 4. SEM images of (a)as-received rice starch powder, (b) freeze-dried gelatinized starch, and (c) freeze-dried retrograded starch.
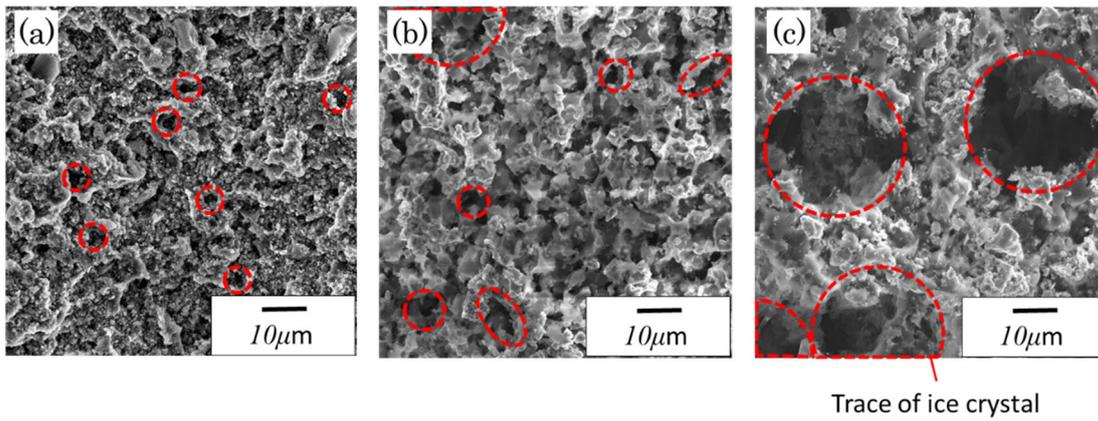
Fig.5

Fig. 5. Microstructures of the green bodies after freeze-drying (a-c): (a) no retrogradation treatment + rapid freezing, (b) retrogradation treatment + rapid freezing, and (c) retrogradation treatment + slow freezing.
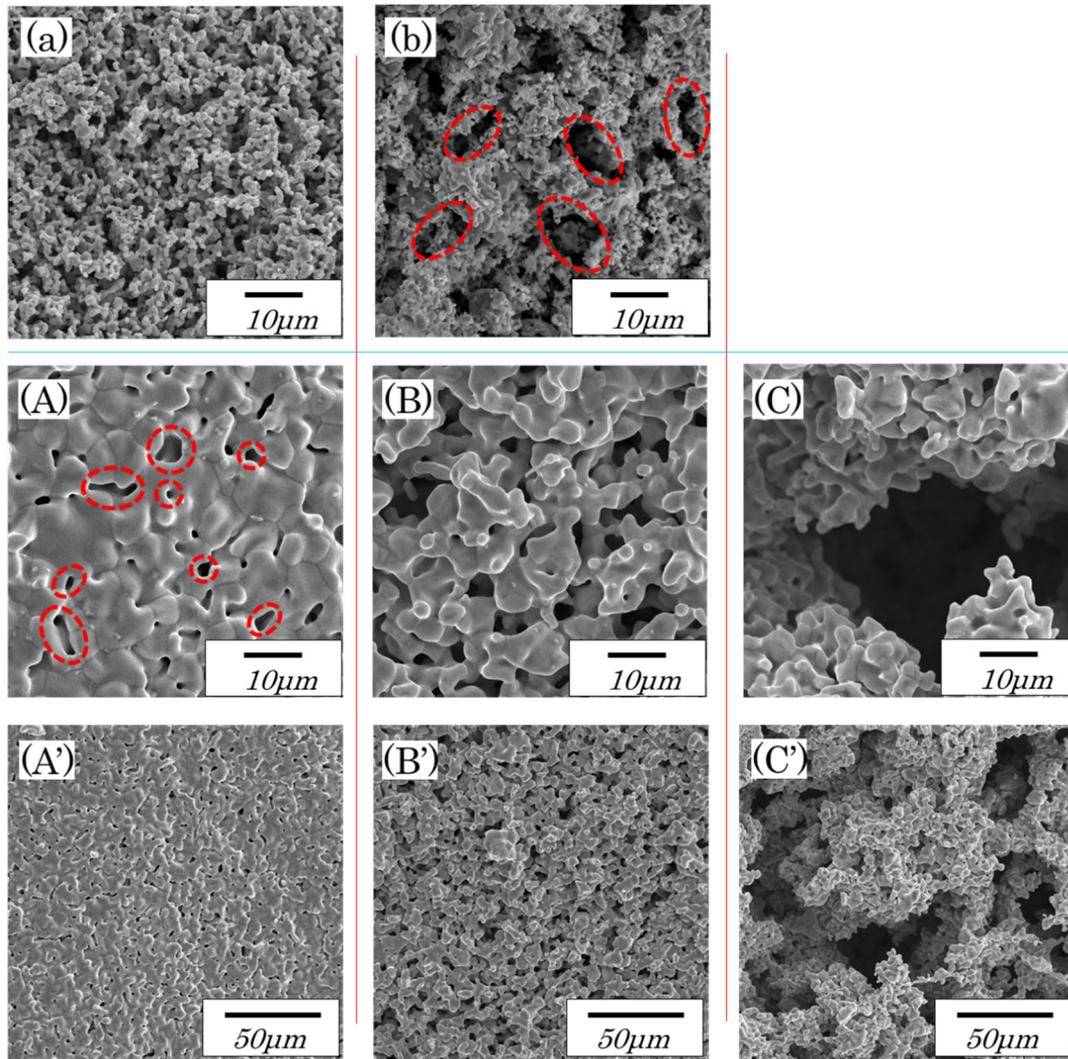
Fig.6

Fig. 6. Microstructures of the porous bodies fired at 900 ˚C (a-b) and 1100 ˚C (A-C): (a, A) no retrogradation treatment + rapid freezing, (b, B) retrogradation treatment + rapid freezing, and (c, C) retrogradation treatment + slow freezing. (A'-C') are the wide-area images of (A-C).
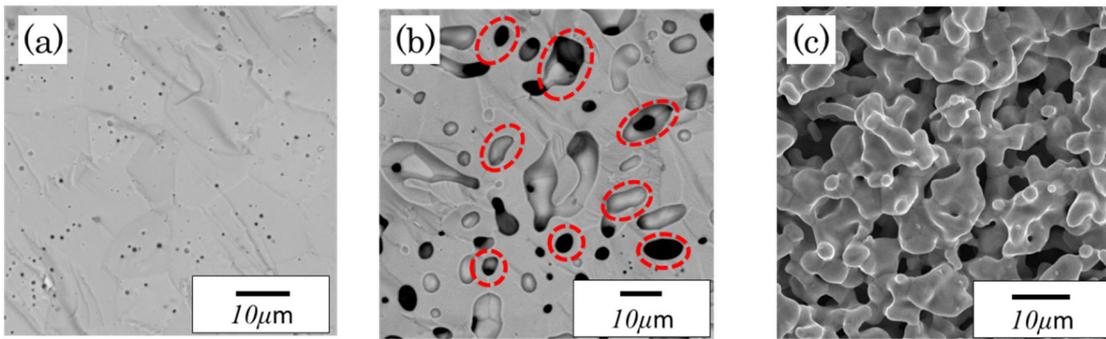
Fig.7

Fig. 7. Microstructures of the BSCFs sintered at 1100 ° C via different preparation methods:
(a)uniaxial pressing without pore forming agent, (b) common sacrificial template method,
and (c) method using the gelatinization-retrogradation phenomena of starch (retrogradation
treatment + rapid freezing). The added amounts of starch in (b) and (c) are both 25 wt.%.
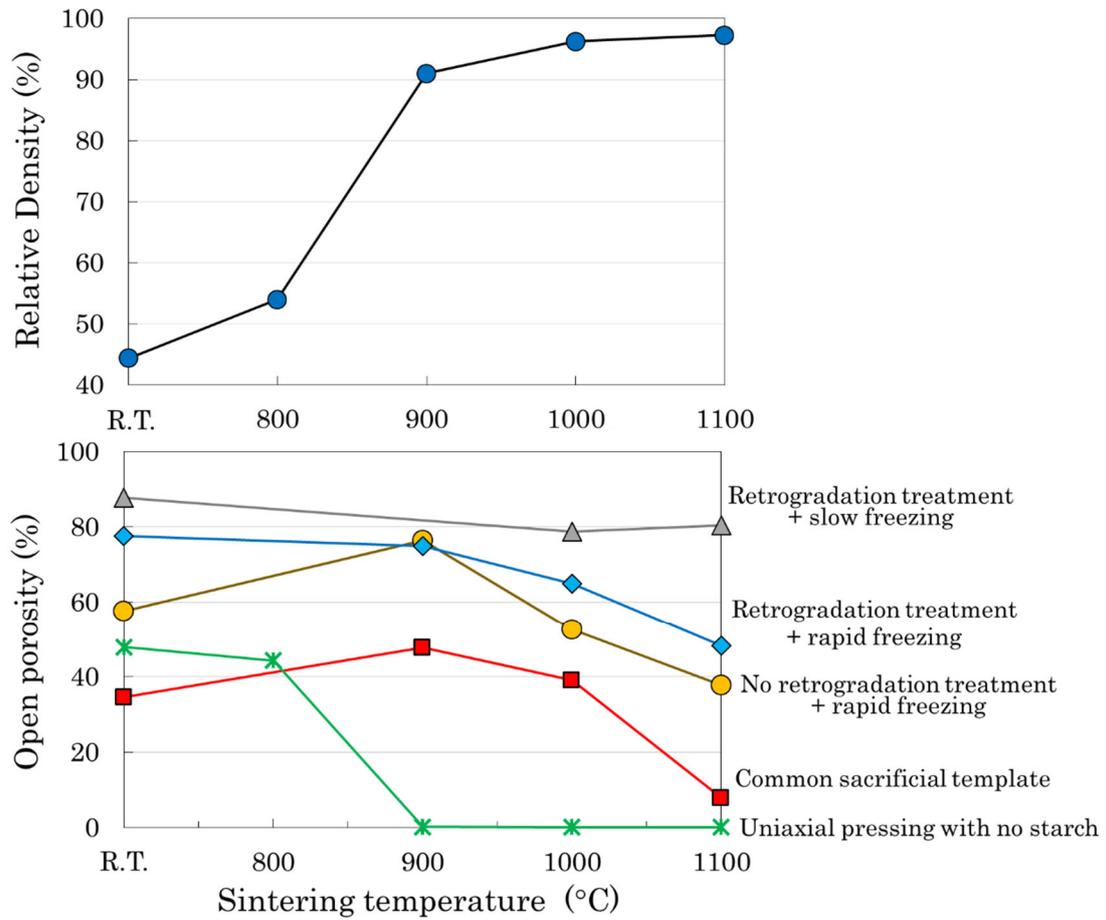
Fig.8

Fig. 8. Sintering properties of the BSCFs: (upper side) Relative density of BSCF with no starch prepared by uniaxial pressing; (lower side) open porosity of the sintered bodies prepared by different methods and conditions.

Table.1

Table 1. The degree of retrogradation progress, porosity and the pore size of green bodies after freeze-drying: (a) no retrogradation treatment + rapid freezing, (b) retrogradation treatment + rapid freezing, and (c) retrogradation treatment + slow freezing.

Sample	(a)	(b)	(c)
Degree of retrogradation progress	small	medium	Large
Porisity (%)	57.6	77.6	87.8
Pore size (μm)	5 <	5～25	10～50

Table.2

Table 2. Porosity, open porosity, pore size, electrical conductivity of the BSCFs sintered at 1100 ° C via different preparation methods: (a)uniaxial pressing without pore forming agent, (b) common sacrificial template method, and (c) method using the gelatinization-retrogradation phenomena of starch (retrogradation treatment + rapid freezing). The added amounts of starch in (b) and (c) are both 25 wt.%.

Sample	(a)	(b)	(c)
Porosity (%)	2.8	21.8	48.4
Open porosity (%)	0	7.9	48.3
Pore size (μm)	< 5.0	5.0 ～ 10.0	5.0 ～ 10.0
Electrical conductivity (S/cm)	26×10^{-3}	1.42×10^{-3}	1.97×10^{-3}